

MULTIVARIATE CALCULATIONS OF THE ELECTRODYNAMIC LINEAR ACCELERATOR WITH A PERMANENT MAGNET SUPPORT

ANDRZEJ WAINDOK, BRONISŁAW TOMCZUK, PAWEŁ PIEKIELNY

Opole University of Technology, Department of Electrical Engineering and Mechatronics, Opole, Poland

e-mail: a.waindok@po.edu.pl; b.tomczuk@po.edu.pl; p.piekielny@po.edu.pl

Multivariate calculations of the electrodynamic accelerator with a permanent magnet support and a ferromagnetic core are presented in the paper. The calculations were made with using the Magnetostatic module of Maxwell/ANSYS software. The purpose of these calculations was to determine the size and location of permanent magnets in terms of maximizing the force acting on the projectile. In the presented paper, three cases have been analyzed. In order to perform a comparative analysis of the obtained results of calculations, dimensions of the rails, projectile and outer dimensions of the core were kept constant.

Keywords: electrodynamic accelerator, multivariate calculations, force calculation, finite element method modelling

1. Introduction

Investigations of electrodynamic accelerators are becoming more and more popular, recently. This is mainly due to the progress in material engineering as well as getting better computer software allowing for more accurate analysis of railgun operation (Chung 2016; Wu *et al.*, 2015; Wang *et al.*, 2016). Numerous research works were devoted to possible construction solutions of the accelerators. They concerned the shape of the cross-section of the rails and projectile, multi-shot systems (two, four, six and even more rails) (Jin *et al.*, 2015; Hric III and Odendaal, 2016; Vincent and Hundertmark, 2013). The aim of such research is increasing the value of magnetic flux density in the area of projectile acceleration and shaping the magnetic field to increase the efficiency of the device (Waindok and Piekielny, 2016). Additional sources of the magnetic field are used to support the initial phase of projectile acceleration. An example of such an external field source is the use of additional circuits: rails, coils as well as permanent magnets (Yamori *et al.*, 2001; McNab, 1999; Gosiewski and Kłosowski, 2008; Engel *et al.*, 2001). The application of permanent magnets to increase the efficiency of devices is widely used, from motors to magnetic bearings (Waindok and Tomczuk, 2017; Wajnert, 2013).

In order to increase the efficiency of railguns, there is a need not only to perform an experimental work, but also to create a proper calculation model which would simulate the physical object with sufficient accuracy (Gieras *et al.*, 2011; Zakrzewski *et al.*, 2009; Kluszczyński and Domin, 2015). The proper mathematical model could be used, for example, in order to investigate the geometry of a given structure in terms of maximizing thrust without increasing the excitation current intensity. Application of multivariate calculations for optimization of a magnetic circuit allows one to consider other possible locations of magnets in terms of maximizing the thrust. For optimization calculations within a defined range of changes, multivariate models are commonly used (Waindok, 2013).

In the paper, results of multivariate calculations for the electrodynamic accelerator with a permanent magnet support and a ferromagnetic core (ICPMR) are presented. The iron core was used in order to focus magnetic field lines while arose from the flow of current through the

electric circuit rail-projectile-rail and from the magnets in the projectile area. Previous studies had shown coincidence between measurements and calculation results for the previously made prototype of the accelerator (Waindok and Pieknielny, 2017). Due to the obtained coincidence, the multivariate calculations were based on the results of the earlier worked out magnetostatic model (in Maxwell software). The non-linear characteristic of the core was measured and taken into account as well.

2. Measurement verification

Our multivariate calculations were done for the model of a previously made accelerator. It is a hybrid construction with two sources of the magnetic field. The picture of the accelerator prototype is presented in Fig. 1a. In Fig. 1b, the dimensioned cross section of the prototype is presented. In order to analyze the dynamic properties of the device, a field-circuit model was developed and verified by measurements.

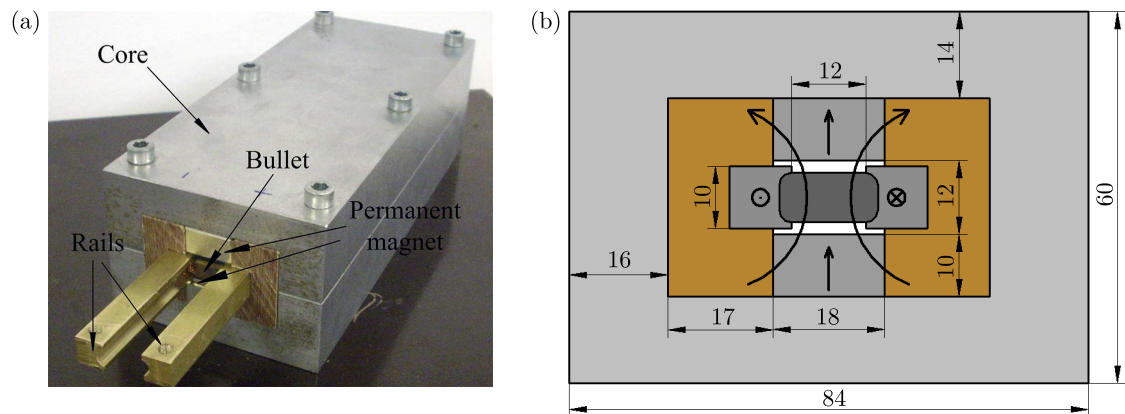


Fig. 1. Electrodynamic accelerator with a ferromagnetic core and permanent magnets: (a) picture of the prototype, (b) cross-section (dimensions in mm)

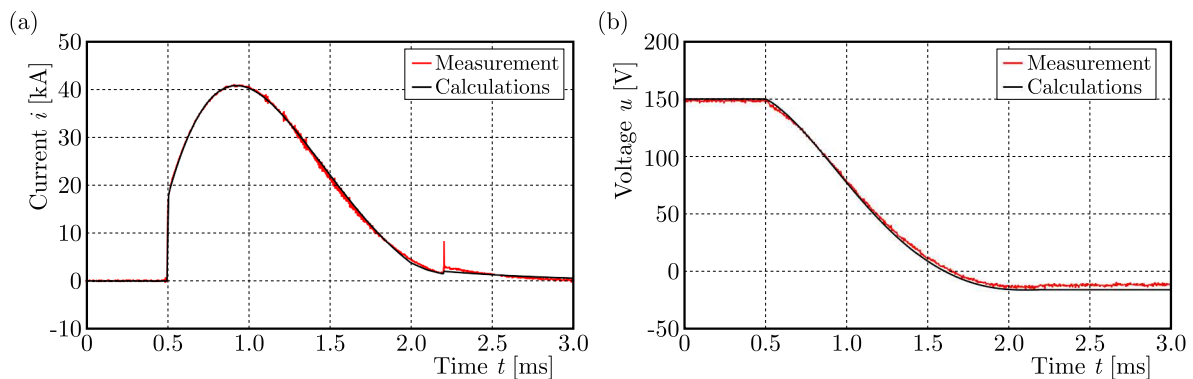


Fig. 2. Measurement verification of the calculation model for $U = 150$ V and $C = 237$ mF: (a) excitation current vs. time, (b) voltage waves

The exemplary verification of the excitation current and voltage waves is shown in Fig. 2 (the following parameters of the power source were assumed: $U = 150$ V and $C = 237$ mF). For the current wave, a very good conformity between calculation and measurement results was observed. The measured voltage wave on the capacitors had a slightly longer time of falling edge of the signal comparing to calculated wave. The negative value of the capacitor voltage was caused by the finite switching-off time of the thyristor ($t_{off} = 100$ μ s). The difference between the muzzle

velocity obtained from the calculation ($v = 118.5$ m/s) and measurements ($v = 117.9$ m/s) did not exceed 1%. It should be mentioned that a very high recurrence of shots for each power supply configuration was obtained. On this basis, a comparative analysis of the multivariate calculations could be carried out.

3. Multivariate calculations

Three cases were analyzed in the presented paper (Fig. 3). The first two cases concerned different locations and dimensions of magnets (in the middle or outer leg of the core). The third case concerned the mixed option. In this case, the dimensions of permanent magnets in the middle leg were fixed (obtained on the basis of calculations from the first case), whereas the dimensions of the magnets in the outer legs of the core were changed. Along with the dimensions of the magnets (w – width, h – height), the inner dimensions of the core were changed. The length of the device $l_T = 300$ mm, length of the iron core $l = 200$ mm as well as the outer dimensions of the core were kept constant for all analyzed cases.

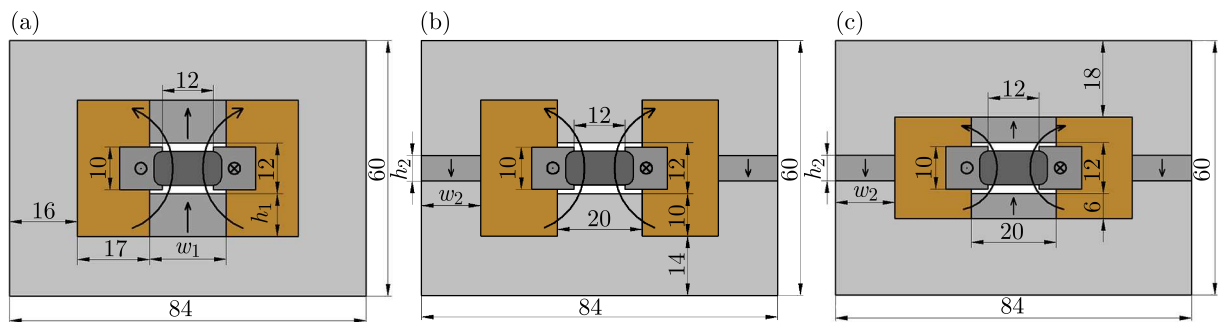


Fig. 3. Cross-section of the electrodynamic accelerator for different locations of permanent magnets: (a) in the middle leg (the first case), (b) in the outer legs (the second case), (c) in the middle and outer legs of the core (the third case)

The calculations were carried out for the fixed projectile position ($z = 150$ mm, middle part of the core) for all analyzed cases and for three values of the current excitation ($I = 10$ kA, 30 kA and 60 kA). The choice of the excitation values was based on the magnetic field analysis (for $I = 10$ kA, the core was non-saturated, while for $I = 60$ kA it was highly saturated). The calculation results for the electrodynamic force vs. width and height of the permanent magnets are presented in Figs. 4-6. The dimensions of the magnets influence the force mostly in the first case. For a lower excitation current value (10 kA), the core material is non-saturated and the force increases nearly linearly with a rise of width and height of the magnets (Fig. 4a). For higher current values, the core material is saturated and the analyzed dimensions of the magnets do not influence the force significantly (Figs. 5a and 6a). For the highest current value, the force increases slightly vs. width of the magnets and decreases vs. its height, which is disadvantageous (Fig. 6a). It is due to the increasing reluctance of the permanent magnet vs. its high and due to nonlinear B/H curve of the core. Based on the obtained results, it can be concluded that in the first case the use of thinner and wider magnets is a better solution.

In the second case (permanent magnets placed in the outer legs), the force increases vs. width and height of magnets regardless of the excitation current. Comparing the results with those obtained for the first case, it can be concluded that the location of magnets in the outer legs of the core is more advantageous.

In the third case (permanent magnets located in each core leg), the dimensions of PMs in the central leg were kept constant. The force vs. outer PM dimensions is similar to that obtained in the 2nd case for relatively low current excitations (Figs. 3c and 4c). In the case of the highest

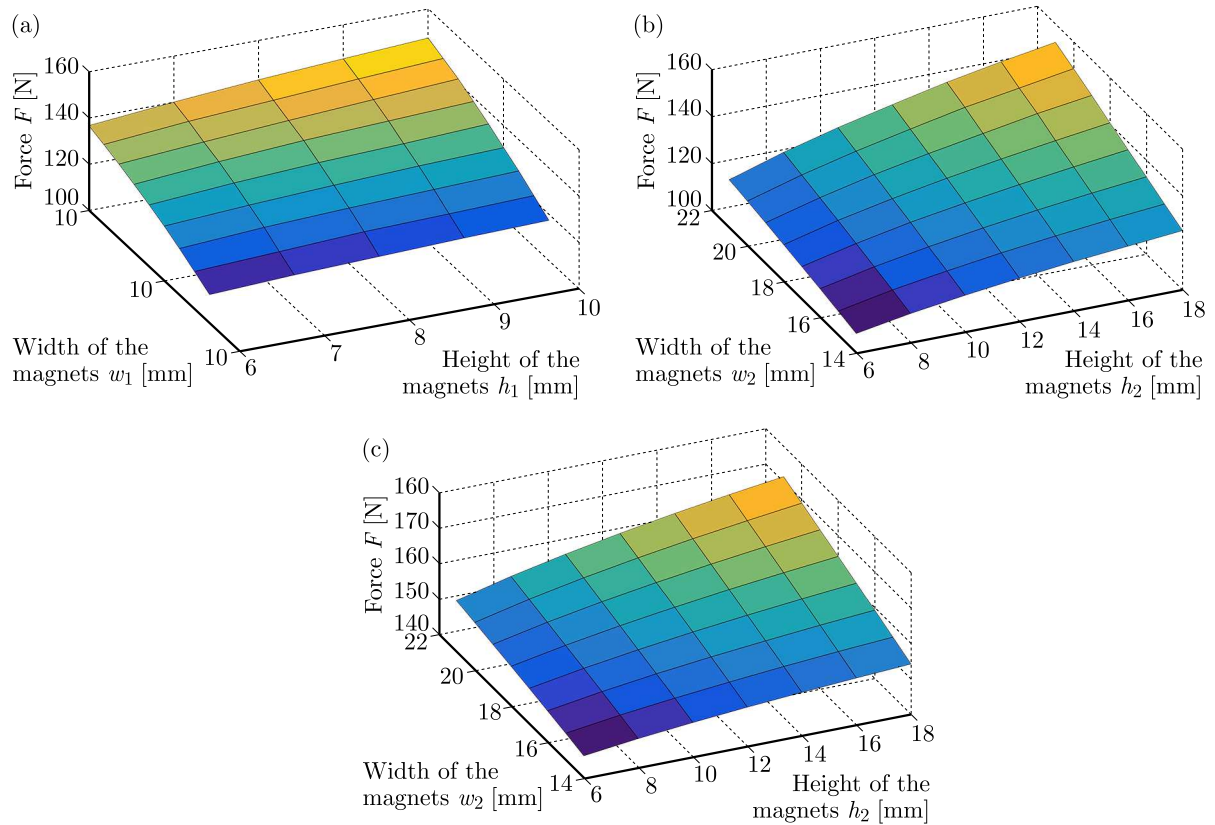


Fig. 4. Electrodynamic force vs. width and height of the permanent magnets for $I = 10$ kA: (a) the first case, (b) the second case, (c) the third case

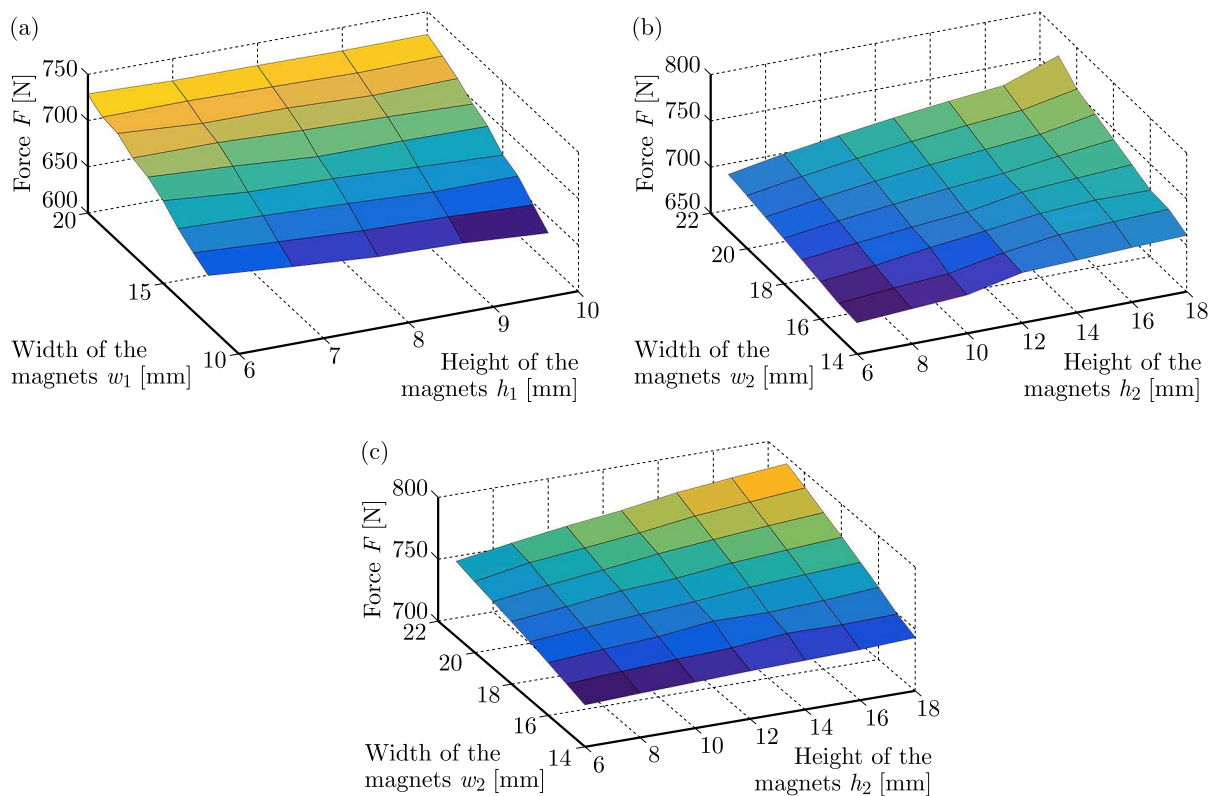


Fig. 5. Electrodynamic force vs. width and height of the permanent magnets for $I = 30$ kA: (a) the first case, (b) the second case, (c) the third case

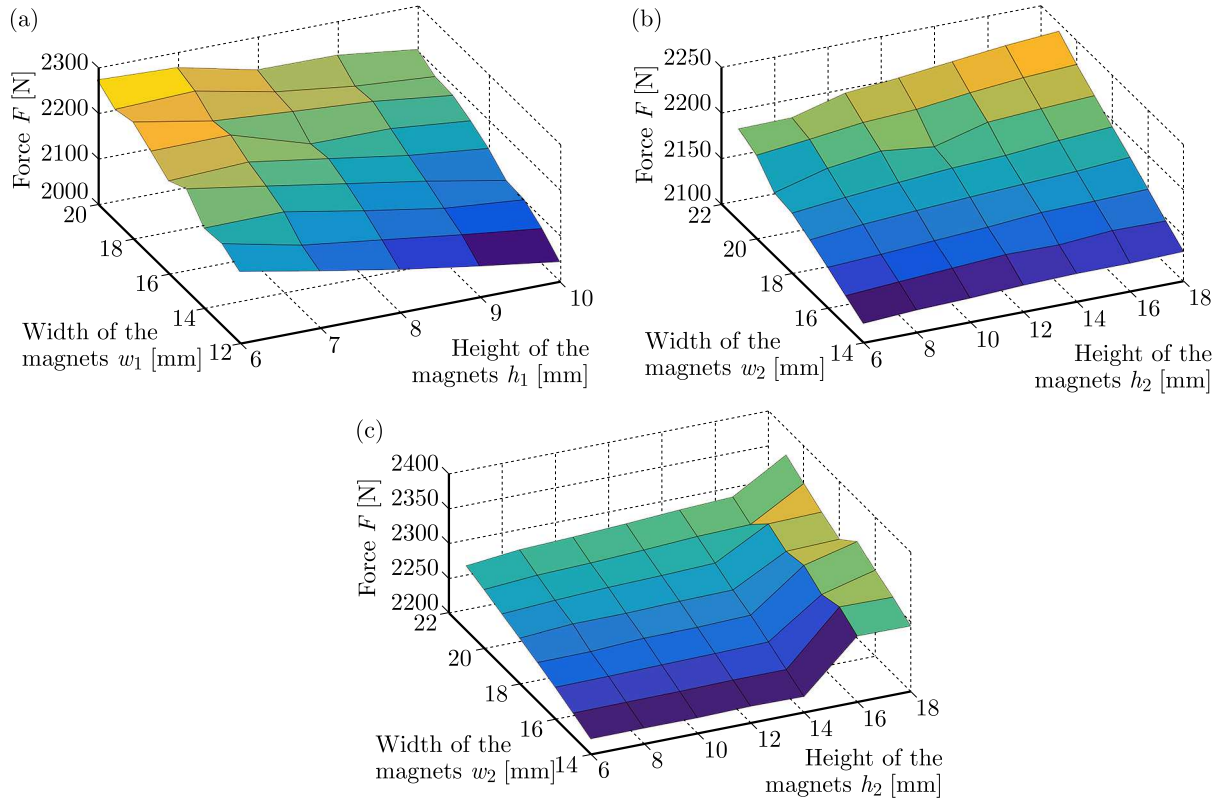


Fig. 6. Electrodynamic force vs. width and height of the permanent magnets for $I = 60$ kA: (a) the first case, (b) the second case, (c) the third case

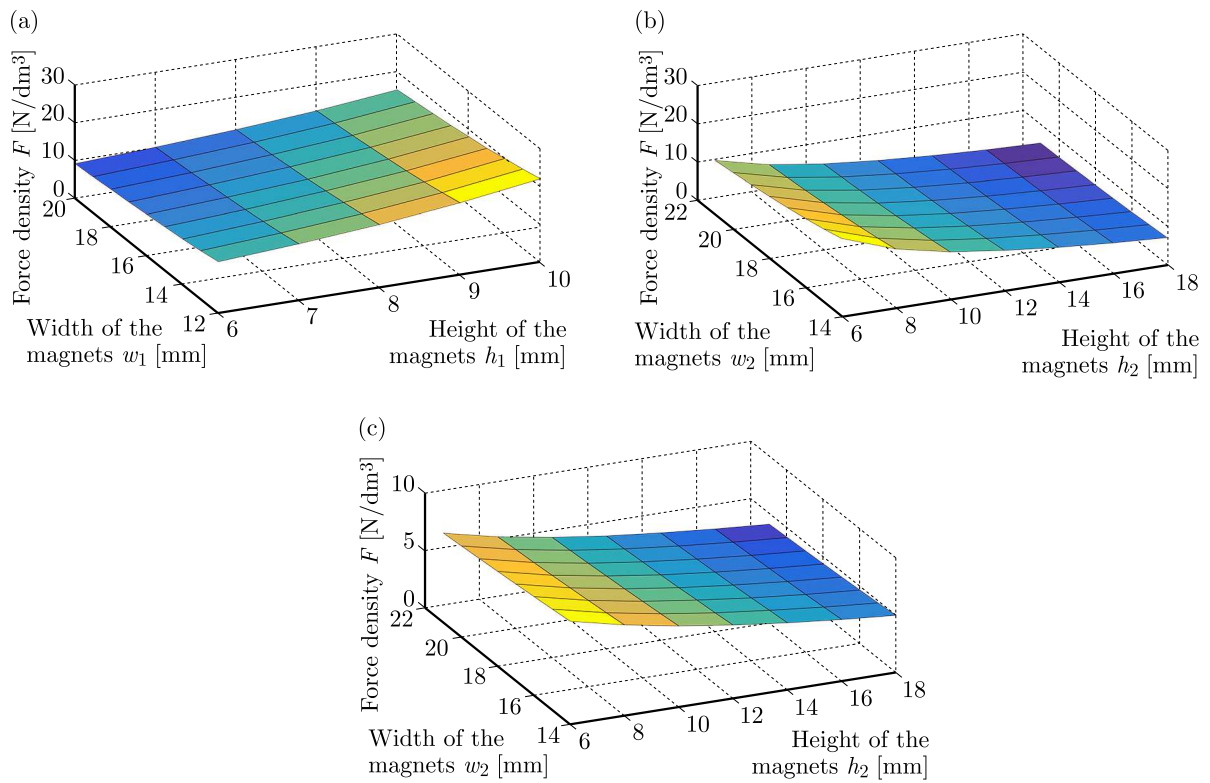


Fig. 7. Value of force density vs. width and height of the permanent magnets for $I = 30$ kA: (a) the first case, (b) the second case, (c) the third case

analyzed current value, we can see a step in the force value vs. magnet high (Fig. 5c). It is due to saturation effects which occur in the core under a high current excitation. The force values are in the third case higher than in the previous analyzed cases.

In order to take into account the material costs for PMs, some calculations of the force density (force over PM volume) were carried out. In Fig. 7, results for the excitation current $I = 30$ kA are presented. In the first analyzed case, the highest force density is observed for relatively high and slim magnets. In the second and third cases, the width of the magnets does not influence the force density significantly. The highest force density value is observed for thin magnets. The lowest values of the force density were obtained in the third case, which means that from the economical point of view, it is the worst solution (the force is less than 10% higher, while the force density is 3 times lower comparing to the first and second analyzed cases).

In Table 1, the obtained results of multivariate calculations for the best solution and the results for the made prototype are presented. The largest percentage increase of the force value was obtained for $I = 10$ kA. The highest force value was obtained for the third case. Comparing to the prototype, the force increased 30% for $I = 10$ kA and 4.5% for $I = 60$ kA.

Table 1. Highest force value for the analyzed cases and for the prototype

Analyzed case	Excitation current	Magnets width	Magnets height	Force
	I [kA]	w [mm]	h [mm]	F_{max} [N]
Prototype	10	18	10	132.16
	30	18	10	716.34
	60	18	10	2256.15
First case	10	20	10	147.17
	30	20	6	728.51
	60	20	6	2272.09
Second case	10	21	18	152.09
	30	21	18	771.40
	60	21	18	2241.43
Third case	10	21	18	171.40
	30	21	18	794.12
	60	21	18	2358.42

Some examples of magnetic flux density distributions for the analyzed cases are presented in Figs. 8-10 ($I = 10$ kA, projectile position $z = 0.15$ m). The highest value of the magnetic flux density is observed in the projectile area (about 2 T for the third case). Such a high value is due to a high current density value and PM field. In the iron parts of the railgun, the magnetic density value is much lower (below 1.5 T).

4. Conclusions

A study of multivariate calculations for different locations and dimensions of magnets for the electrodynamic accelerator (railgun) with permanent magnets support is presented in the paper. The obtained results allow one to formulate some conclusions:

- With an increase of the core material saturation, the effect of permanent magnets on the value of the magnetic force is minor (Table 1).
- The location of the magnets affect the force value. Better results were obtained for the location of magnets in the outer legs of the core.

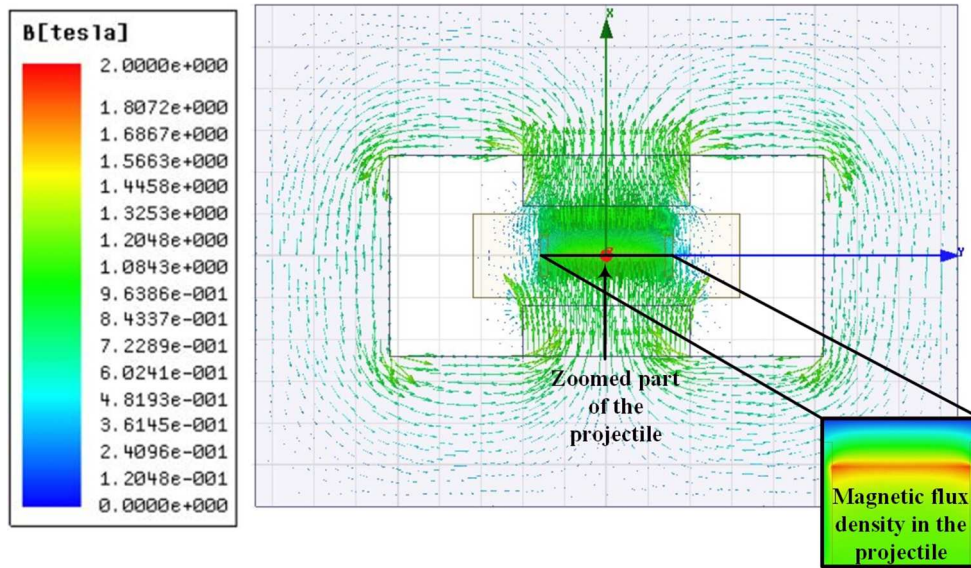


Fig. 8. Magnetic flux density distribution in the cross section of the railgun for the best result in the first case ($h = 6$ mm and $w = 20$ mm, $I = 10$ kA)

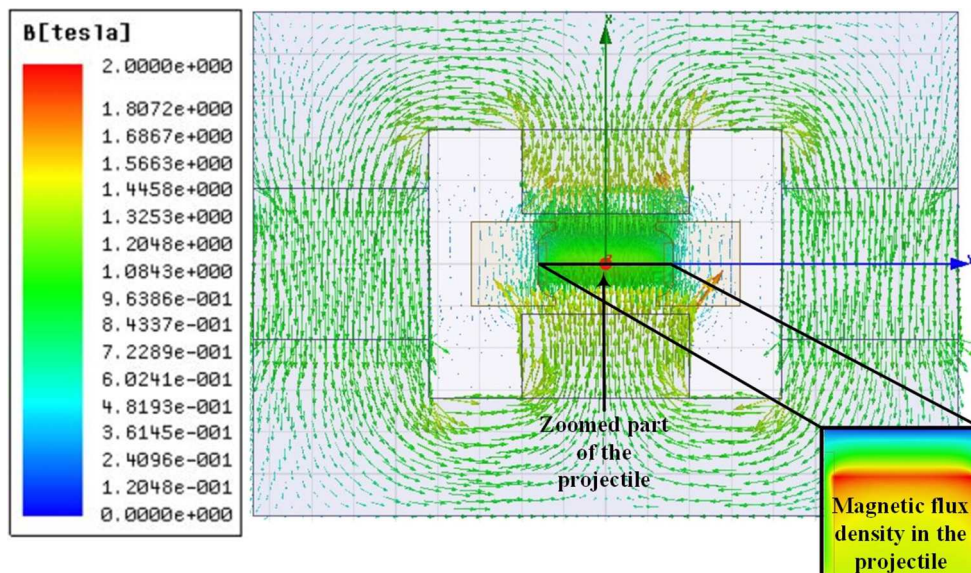


Fig. 9. Magnetic flux density distribution in the cross section of the railgun for the best result in the second case ($h = 18$ mm and $w = 21$ mm, $I = 10$ kA)

- The best effects were obtained for the third case where the force increased 30% (for $I = 10$ kA) and 4.5% (for $I = 60$ kA) comparing to the prototype.
- In the first case, the width of the magnets influences the force more significantly than their height.
- In the second and the third cases, with an increase of the height and width of the magnets, the force increased regardless of the excitation current.
- The force density values are highest for the first and the second cases (3-times higher than in the third case). Considering the slight increase (below 10%) in the force value, the third case is less substantiated from the economical point of view than the first two cases.
- The analyzed steel core concentrates the magnetic field lines in the projectile area and shields magnetically the rails.

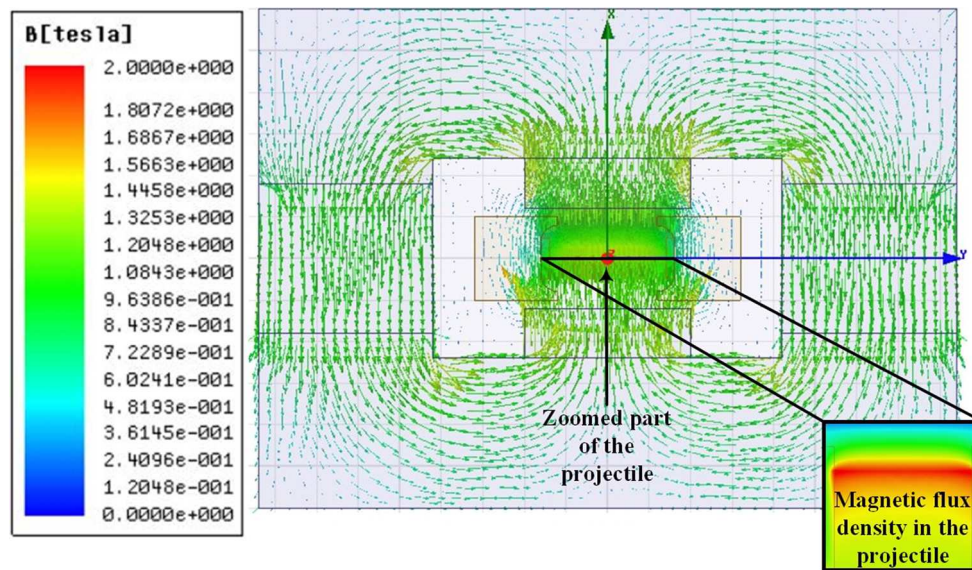


Fig. 10. Magnetic flux density distribution in the cross section of the railgun for the best result in the third case ($h = 18\text{ mm}$ and $w = 21\text{ mm}$, $I = 10\text{ kA}$)

The results obtained within the presented work will be used in the development of an improved railgun construction. Permanent magnets placed in the outer legs of the core could be used in a hybrid construction of a railgun for improving the initial acceleration of the projectile.

References

1. CHUNG S.S.M., 2016, Parametric study of possible railgun radiation in postfire stage, *IEEE Transactions on Plasma Science*, **44**, 6, 980-990
2. ENGEL T.G., SURLS D., NUNNALLY W.C., 2001, All-electric rifle-caliber launcher with permanent magnet augmentation, *IEEE Transactions on Magnetics*, **37**, 6, 3934-3940
3. GIERAS J.F., PIECH Z.J., TOMCZUK B., 2011, *Linear Synchronous Motors*, CRC Press, Taylor & Francis Group, New York
4. GOSIEWSKI Z., KŁOSOWSKI P., 2008, Support of work of electromagnetic gun by using permanent magnets, *Bulletin of the Military University of Technology*, **57**, 3, 87-95
5. HRIC III G.R., ODENDAAL W.G., 2016, Improving Start-up contact distribution between railgun armature and rails, *IEEE Transactions on Plasma Science*, **44**, 7, 1202-1207
6. JIN L., LEI B., ZHANG Q., ZHU R., 2015, Electromechanical performance of rails with different cross-sectional shapes in railgun, *IEEE Transactions on Plasma Science*, **43**, 5, 1220-1224
7. KLUSZCZYŃSKI K., DOMIN J., 2015, Two module electromagnetic launcher with pneumatic assist modelling, computer simulations and laboratory investigations, *COMPEL*, **34**, 3, 691-709
8. McNAB I.R., 1999, The STAR railgun concept, *IEEE Transactions on Magnetics*, **35**, 1, 432-436
9. VINCENT G., HUNDERTMARK S., 2013, Using the hexagonal segmented railgun in multishot mode with three projectiles, *IEEE Transactions on Plasma Science*, **41**, 5, 1431-1435
10. WAINDOK A., 2013, *Modeling and Measurement Verification of Characteristics for the Permanent Magnet Tubular Linear Actuators*, Oficyna Wydawnicza Politechniki Opolskiej, Opole
11. WAINDOK A., PIEKIELNY P., 2016, Calculation models of the electrodynamic accelerator (railgun), *Przełąd Elektrotechniczny*, **92**, 9, 246-249

12. WAINDOK A., PIEKIELNY P., 2017, Transient analysis of a railgun with permanent magnets support, *Acta Mechanica et Automatica*, **11**, 4, 302-307
13. WAINDOK A., TOMCZUK B., 2017, Reluctance network model of a permanent magnet tubular motor, *Acta Mechanica et Automatica*, **11**, 3, 194-198
14. WAJNERT D., 2013, Comparison of magnetic field parameters obtained from 2d and 3d finite element analysis for an active magnetic bearing, *Proceedings of International Symposium on Electrodynamic and Mechatronic Systems*, 73-74
15. WANG G.H., XIE L., HE Y., SONG S.Y., GAO J.J., 2016, Moving mesh FE/BE hybrid simulation of electromagnetic field evolution for railgun, *IEEE Transactions on Plasma Science*, **44**, 8, 1424-1428
16. WU S., WANG X., CUI S., ZHAO W., 2015, Risk evaluation for hybrid excitation compulsator, *IEEE Transactions on Plasma Science*, **43**, 5, 1410-1414
17. YAMORI A., ONO Y., KUBO H., KONO M., KAWASHIMA N., 2001, Development of an induction type railgun, *IEEE Transactions on Magnetics*, **37**, 1, 470-472
18. ZAKRZEWSKI K., TOMCZUK B., KOTERAS D., 2009, Amorphous modular transformers and their 3D magnetic fields calculation with FEM, *COMPEL*, **28**, 3, 583-592

Manuscript received October 25, 2018; accepted for print December 13, 2019